Assessing the Effects of Residual Stresses on the Fatigue Strength of Spot Welds

Residual stress at the nugget's edge was taken into consideration in the evaluation of fatigue strength for spot welds of various shapes and dimensions

BY D. H. BAE, I. S. SOHN, AND J. K. HONG

ABSTRACT. This paper presents a method for fatigue strength assessment of spot welds, which incorporates the effects of welding residual stress. Residual stress analysis with a welding thermal history was evaluated first, and then stress analysis for fatigue was performed.

First, the residual stresses of spot welds were calculated using a nonlinear finite element analysis (FEA). To validify the FEA results, the calculated residual stresses were compared to those measured by X-ray diffraction. The residual stress distributions showed good agreement between calculations and measurements. Then, to evaluate the fatigue strength of spot welds, stress analyses were performed under tensile loading on various dimensions and shapes of spot welds.

Based on the results, the stress amplitude ($\sigma_{a\text{-}res}$), which took into consideration welding residual stress at the nugget edge of a spot weld, was calculated using a modified Goodman equation. Using the stress amplitude $\sigma_{a\text{-}res}$ at the nugget edge, the load range (ΔP)–fatigue life (N_f) relations from the fatigue tests can be replaced by the $\sigma_{a\text{-}res}$ -N_f relations.

It was found the proposed stress amplitude ($\sigma_{a\text{-}res}$) provided a systematic and accurate evaluation of fatigue strength of spot-welded joints with various dimensions and shapes.

Introduction

Fatigue strength of spot-welded joints affects the structural rigidity and durability of spot-welded structures, and thus it is an important factor in determining safety and structural integrity. To determine design criteria for long fatigue life for spot-welded structures, accurate stress analysis and systematic fatigue strength assessment are needed. Since it is very difficult to determine directly the fatigue design criteria for actual structures, it is a typical practice to assess fatigue strengths using mock-up specimens with structural and mechanical characteristics similar to the actual structures (Refs. 1, 2).

Many investigators have numerically and experimentally assessed fatigue strength and provided considerable data on the fatigue strength of various spot-welded joints (Refs. 2, 3). To apply the data into the fatigue design of actual spot-welded thin sheet structures, welding residual stress should be properly considered since it affects fatigue crack initiation and propagation at the nugget edge of a spot weld. Nevertheless, there are very few fatigue strength assessments that consider welding residual stress because welding residual stress analysis is quite complicated (Refs. 4–6).

Research on welding residual stress analysis is summarized as follows: Tsai et al. (Ref. 7) proposed an FEA model for weld nugget generation in the resistance spot welding process. Anastassiou et al. (Ref. 8) performed an experimental investigation on welding residual stress and microstructure distribution in spot-welded steel sheets and showed residual stress distribution was high tensile stress at the center and compressive stress near the notch root where a fatigue crack initiates. Nied (Ref. 9) investigated the FEA modeling of the resistance spot welding process for numerical stress analysis. In this investigation, he proposed material properties be considered in modeling the weld nugget and the methodology for modeling the electrode. Kim and Eager (Ref. 10) investigated transient temperature response during spot welding using high-speed cinematography and infrared emission monitoring. Huh and Kang (Ref. 6) developed a three-dimensional (3-D) FEA model for electro-thermal analysis of the resistance spot welding process.

For fatigue analyses, the stress categories are generally evaluated by using a nominal stress, a structural hot spot stress, and a notch stress with consideration of stress concentration effects. The choice of stress category depends on the method used to express the fatigue strength data in the fatigue assessment (Ref. 11). Among these categories, nominal stress and notch stress can be considered as the mechanical parameters for fatigue strength assessment of a spot-welded joint.

In this paper, the maximum stress range at the edge of the spot weld nugget, instead of nominal stress, was correlated with the fatigue strength of a spot weld. A nonlinear FEA was conducted to simulate welding residual stress generated by thermal cycles during the spot welding process and then the calculated residual stresses were compared with experimental data measured by the X-ray diffraction method to validate the numerical results. Based on the results, the stress amplitude ($\sigma_{a\text{-}res}$) with consideration to welding residual stress at the edge of the spot weld nugget was calculated using a modified Goodman equation. Then the fatigue load range (ΔP)-fatigue life (N_f) relations obtained from the fatigue test for spot welds of various dimensions and shapes were placed into the stress amplitude ($\sigma_{a\text{-}res}$)-fatigue life (N_f) relation.

Welding Residual Stress Analysis

FEA Model and Assumptions

Spot welding is a material joining technology using electrical resistance heat of

KEY WORDS

Spot Welds
Fatigue Strength
Residual Stress
Maximum Principal Stress
Finite Element Method
X-Ray Diffraction

D. H. BAE (bae@yurim.skku.ac.kr) *is Professor, School of Mechanical Engineering, SungKyunKwan University, Suwon-City, Kyunggi-Do, South Korea. I. S. SOHN* (issohn@mail.osan-c.ac.kr) *is Professor, Dept. of Machine Design Engineering, Osan College, Osan-City, Kyunggi-Do, South Korea. J. K. HONG is Research Scientist, Battelle Memorial Institute, Columbus, Ohio.*

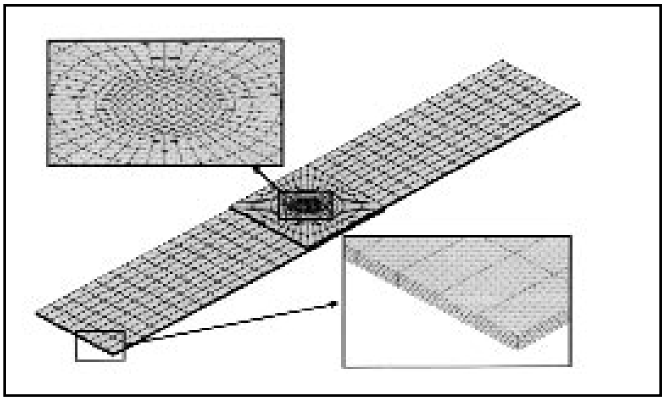

Fig. 1 — Three-dimensional nonlinear FEA model used for welding residual stress analysis of a spot-welded joint.

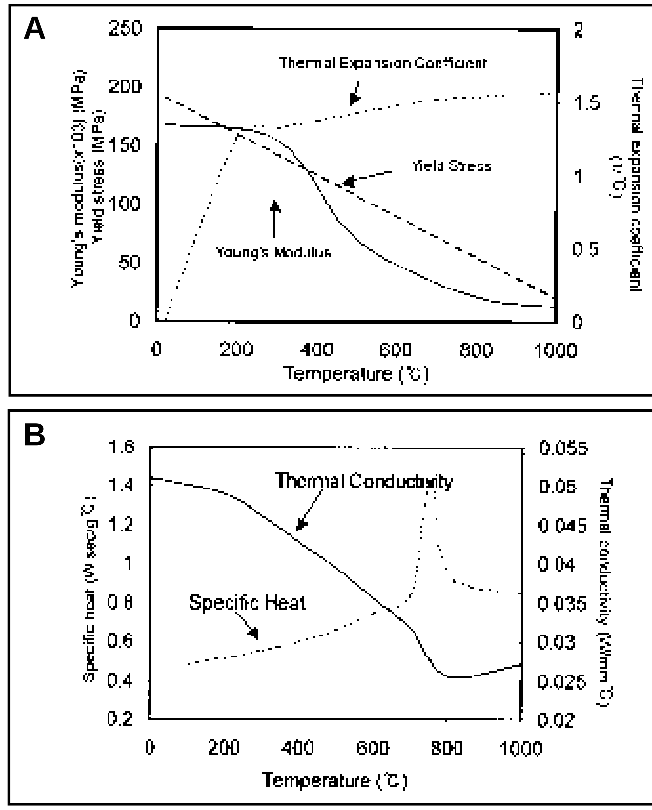

Fig. 2 — Temperature-dependent material properties employed in nonlinear FEA. A — Mechanical properties; B — thermal properties.

metallic material. During the resistance spot welding process, expansion and shrinkage of the material occurs due to the thermal cycle. Thus, welding residual stress and electrode indentation remain at the spot weld after the spot welding process.

In this paper, welding residual stresses were analyzed both numerically and experimentally. The numerical analysis procedure for determining welding residual stress on spot welds consists of two parts: one is thermal analysis and the other is mechanical analysis. Once the temperature is calculated from thermal analysis, then the mechanical analysis is conducted with the corresponding temperature histories.

The 3-D FEA model employed in the present work is shown in Fig. 1. Solid brick elements were used for upper and lower plate modeling. The total number of elements and nodes are 4300 and 6151, respectively. The weld nuggets were prepared using multipoint constraints of the element nodes on the contact surface to prevent the incursion between the upper and lower elements during the welding process. A sufficiently fine mesh at the nugget was generated to obtain more accurate results. Each plate was divided into four layers to show the nugget generation process. The boundary conditions of the FEA model were the same as those of the test condition.

The material used for both FEA model and fatigue specimen is a cold-rolled sheet steel called SPCE, widely used for an automobile body. The chemical composition and mechanical properties of the specimen at room temperature are given in Tables 1 and 2, respectively. The spot welding condition was defined as the same as in an actual automobile body assembly facility, which is described in Table 3. The temperature-dependent material properties applied for the FEA are shown in Fig. 2 (Ref. 12). The yield strength of SPCC rapidly decreased when the temperature reached more than 400°C and the specific heat increased with temperature but rapidly changed near 800°C. The thermal expansion coefficient linearly increased to 200°C and thermal conductivity decreased at more than 200°C and slightly increased at more than 800°C. Young's modulus decreases almost linearly with temperature.

Generally, a welding nugget is generated by thermal cycles of heating and cooling of the spot welding process. In this analysis, however, nugget temperature distributions were calculated using the heat block element within *ABAQUS*, which can be referred to Huh and Kang (Ref. 6) and RWMA (Ref. 13). *ABAQUS,* a commercial FEA package, was employed for the transient temperature and subsequent residual stress analysis.

Results of Numerical Residual Stress Analysis

The temperature profiles taken at the nugget center, the nugget edge, and locations 5 mm away from the nugget center of the inner and outer surfaces of the plate are shown in Fig. 3. The peak temperature was around 1300°C at the nugget center of the inner surface, 700°C at the nugget center of the outer surface, and 400°C at the nugget edge of both inner and outer surfaces.

The temperature distribution on the

Table 1 — Chemical Composition of SPCC (wt-%)

	C	Si	Mn	P	S	Ni	Al	Fe
SPCC	0.12	0.01	0.127	0.015	0.007	0.025	0.045	Rem

Table 2 — Mechanical Properties of SPCC

	Tensile Strength (MPa)	Yield Strength (MPa)	Elongation (%)
SPCC	307	168	47

Table 3 — Welding Condition of SPCC

	Electrode Force (N)	Welding Current (kA)	Welding Time (Cycles)
Welding condition	1962	8.3	15

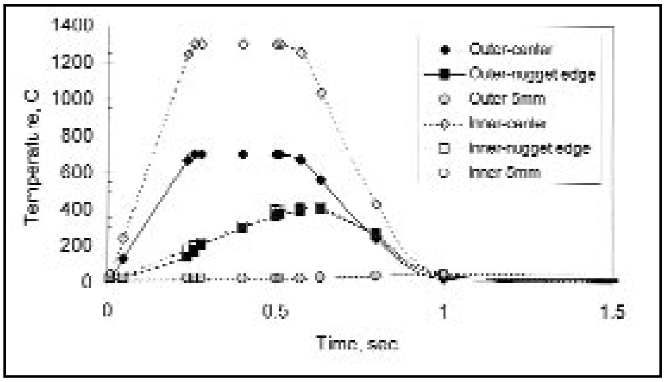

Fig. 3 — Temperature profiles on the inner and outer surfaces of the plate.

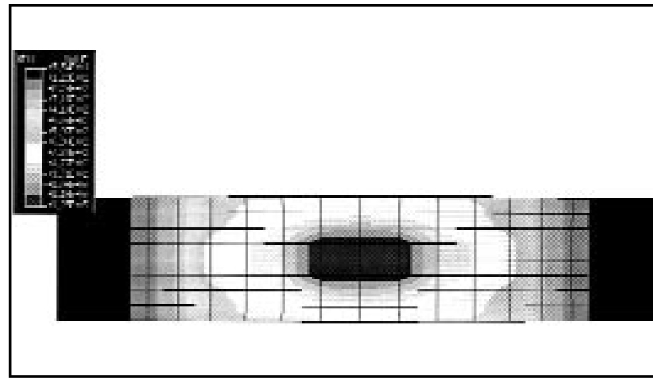

Fig. 4 — Temperature distribution on the nugget cross section.

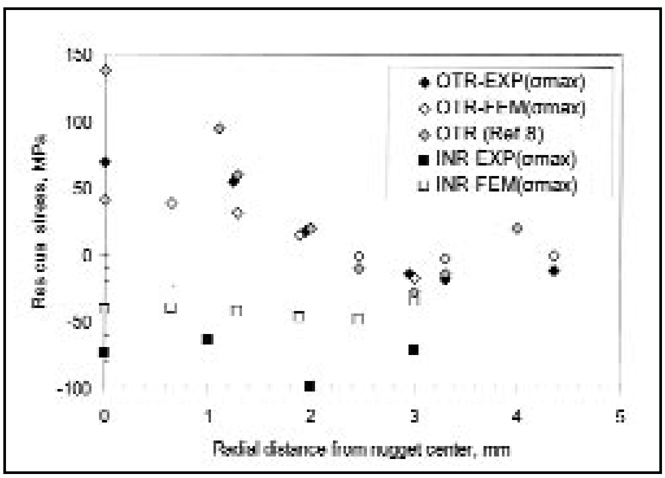

Fig. 5 — Welding residual stress distributions of the spot weld (outer surface, OTR; inner surface, INR; experimental data, EXP; FEA results, FEM).

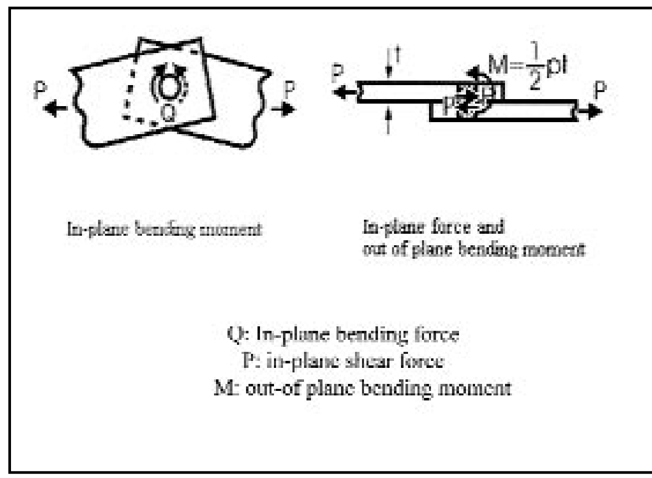

Fig. 6 — Inner forces acting on the nugget.

outer surface is lower than on the inner surface due to heat transfer from the outer surface of the nugget to both upper and lower electrodes, which are cooled by circulating water. However, both inner and outer surface temperature distributions at the nugget edge show similar results. Figure 4 shows the temperature distribution on the nugget cross section after the welding nugget has been generated.

In general, since fatigue crack initiation occurs at the nugget edge on the inner surface of the loading side, it would be reasonable to look at the stress at the fatigue crack initiation location to assess the fatigue strength of spot welds. Therefore, in this investigation, welding residual stresses at the nugget edge on the inner surface were analyzed both numerically and experimentally.

Calculated residual stresses at the nugget center show +40 MPa (in tension) and –40 MPa (in compression) on the outer and inner surface, respectively. Also, calculated welding residual stresses at the nugget edge are approximately –17 MPa (in compression) and –38 MPa (in compression) on the outer and inner surface, respectively. Welding residual stresses on the outer surface show high tension at the nugget center and compression around the nugget edge.

Measurement of Residual Stresses Using X-Ray Diffraction Method

To validate the numerical results, welding residual stresses were also experimentally analyzed using the X-ray diffraction method. The X-ray diffraction unit used is the MSF-2M type by Rigaku Co. of Japan. Welding residual stresses were measured with the following conditions and procedures: the projected area was 2 mm^2 and the X-ray was exposed to the inner and outer surfaces of the nugget area in four different angles and three times, respectively. Their mean values were applied to calculate welding residual stresses using the $\sin^2\theta$ method. Note that in the process of cutting off the upper plate of the spot-welded joint under wet conditions, machining can influence welding residual stresses at the nugget edge on the inner surface of the lower plate. Since its influence is believed to be insignificant, it was not considered in this study.

Comparison of the Numerical and Experimental Results

The calculated welding residual stresses on the inner and outer surface of spot-welded joints were compared to measured values and data by Anastassiou, et al. (Ref. 8) in Fig. 5. Welding residual stresses measured in experiment were about +70 MPa (in tension) at the outer surface of the nugget center and –75 MPa (in compression) at the inner surface. In the numerical analysis, the values were approximately +40 MPa (in tension) at the outer surface of the nugget center and –40 MPa (in compression) at the inner surface of the nugget center. Both the numerical and the experimental results showed high tension at the outer surface of the nugget center and compression around the nugget edge. Calculated and measured residual stresses at the nugget edge on outer surface were –17 MPa (in compres-

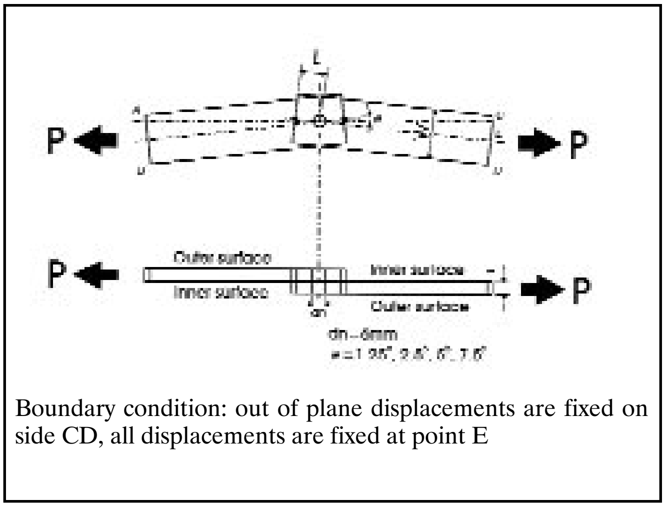

Fig. 7 — Stress analysis model of IB-type spot-welded joint.

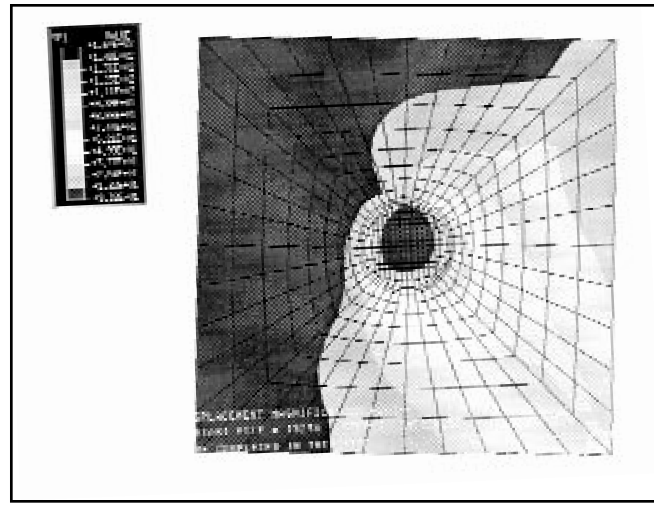

Fig. 8 — Stress distribution around the spot weld of IB-type spot-welded lap joint subjected to tensile shear load.

sion) and –14 MPa (in compression), respectively. Also, calculated and measured residual stresses at the nugget edge on the inner surface were –38 MPa (in compression) and –70 MPa (in compression), respectively.

Such a discrepancy between the numerical and experimental values for welding residual stresses may be attributed to the difference between the conditions of the numerical analysis and the experiment. The nugget metal was actually pressed out by the electrode force and thermal expansion. However, such actual welding conditions and various thermal and physical properties were neglected in the process of the FEA. Also, the effect of phase transformation during the welding process and the release of residual stress when cutting off the plate with wet machining were not considered in the FE analysis. In spite of the discrepancy, the residual stress distributions show reasonable agreement between the calculations and measurements.

Stress Analysis Considering the Welding Residual Stress

Stress Analysis Model

In order to evaluate the fatigue strength of spot-welded joints, stress analysis was also performed. The model is a spot-welded bus window pillar joint sustaining in-plane bending force by warping of the body structure. When the external tensile shear load is applied to the in-plane bending (IB) type single spot-welded lap joint, three kinds of internal forces act on the spot-weld: in-plane shear force (P), in-plane bending force (Q), and out-of-plane bending moment (M), as illustrated in Fig. 6. These internal forces give a very complicated pattern of deformation (Ref. 15). Fatigue cracks are generally generated at the nugget edge on the inner surface and propagated to the outer surface of the plate by this deformation mechanism and stress concentration. Therefore, it is very important to calculate the accurate stress and strain distributions around the weld nugget for a reasonable fatigue strength assessment.

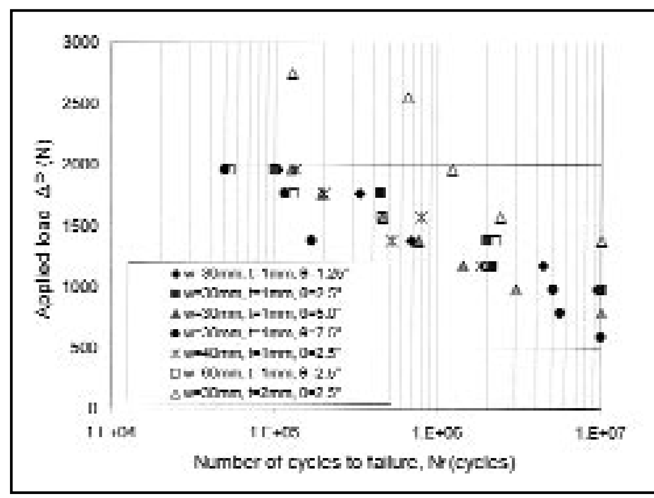

Fig. 9 — ΔP-N_f relation of IB-type spot-welded lap joints.

In this study, a 3-D FE model was used to calculate the stress distribution. Dimensions of the reference model are plate thickness, *t*, 1 mm; plate width, *w*, 30 mm; specimen lapped length, *2L*, 30 mm; and joint angle between upper and lower plate, θ, 2.5 deg. Three-dimensional solid brick elements were used for the FEA model. The total numbers of elements and nodes used were 1164 and 1992, respectively. The upper and lower plates had only one layer of solid brick element and the weld nugget area had a refined mesh. The nugget size was modeled with the same diameter of electrode used in industrial fields, and the weld nugget was modeled using multipoint constrains for the nodes of the upper and lower elements on the contact surface. Boundary conditions and load conditions were assumed as the same as those for the fatigue tests. Fatigue strength was actually assessed with the mechanical parameter and it was calculated with the actual load applied to each fatigue specimen. *ABAQUS*, a commercial FEA package, was used for the stress analysis. The stress analysis model is drawn in Fig. 7.

Results of Stress Analysis

Stress distributions around the weld of IB-type spot-welded joint subjected to tensile shear load are shown in Fig. 8. It shows stress concentration occurs at the nugget edge on the loading side of the plate and ranges from –20 to 40 deg, which is affected by the joint angle. When the joint angle was more than 5 deg, tensile stresses were simultaneously generated at the nugget edge in the opposite side as well as in the loading side. This phenomenon is due to the fact that out-of-plane bending and in-plane bending deformation increase with the joint angle increases. It is known that other geometrical factors such as plate thickness and

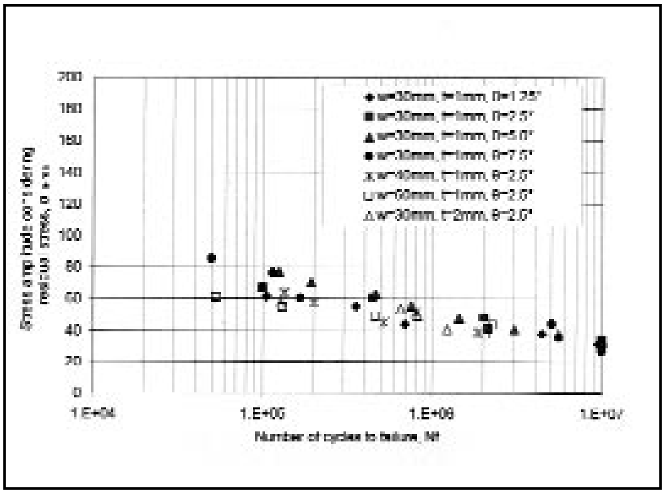

Fig. 10 — Representation in the $\Delta\sigma_{a\text{-}res}$-$N_f$ relation of various IB-type spot-welded lap joints.

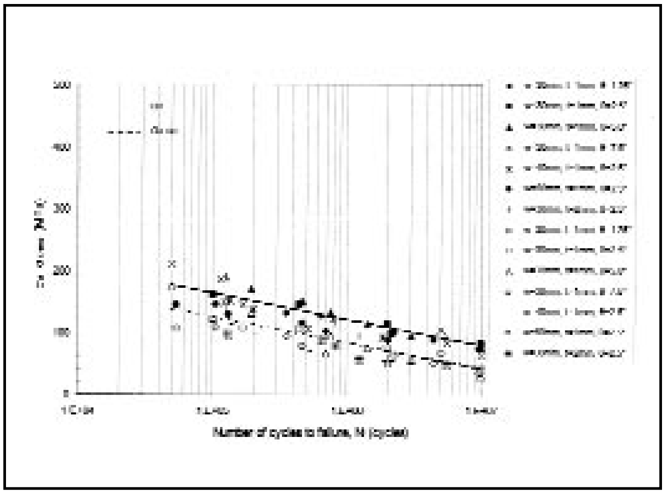

Fig. 11 — Comparison of the σ_a-N_f relation and the $\sigma_{a\text{-}res}$-N_f relation of various IB-type spot-welded lap joints.

width also affect stress concentration around the nugget edge (Ref. 16).

Calculation of the Stress Amplitude Considering Welding Residual Stress

Among the stress categories, the nominal stress and the notch stress can be considered as mechanical parameters for systematic fatigue strength assessment of spot-welded joints. As mentioned previously, nominal stress ($\sigma_n = P/W\cdot t$, W is width of plate, and t is plate thickness) of the plate is considerably influenced by geometrical factors such as the plate thickness and the width. Therefore, it is proposed to use the maximum principal stress at the nugget edge on the inner surface of IB-type spot-welded lap joints. The stress amplitude ($\sigma_{a\text{-}res}$), which considers welding residual stress, was calculated using the modified Goodman equation that follows.

$$\frac{\sigma_a}{S_e} + \frac{\sigma_{mean}}{S_u} = 1, \qquad (1)$$

$$where\ \sigma_a = \frac{\sigma_{max} - \sigma_{min}}{2};$$

$$\sigma_{mean} = \frac{\sigma_{max} + \sigma_{min}}{2}$$

S_e is fully reversed fatigue strength at a given number of cycles; S_u is ultimate stress; σ_{min} and σ_{max} denote the minimum and maximum stresses, respectively. The modified Goodman equation considering welding residual stress, which was proposed in this study, can be written as

$$\frac{\sigma_{a\text{-}res}}{S_e} + \frac{\left(\sigma_{mean} + \sigma_{res}\right)}{S_u} = 1 \qquad (2)$$

where $\sigma_{a\text{-}res}$ and σ_{res} are the stress amplitudes, which consider welding residual stress and welding residual stress at the nugget edge of the spot weld, respectively. In Equation 2, $\sigma_{a\text{-}res}$ is defined as

$$\sigma_{a\text{-}res} = S_e\left\{1 - \frac{\left(\sigma_{mean} + \sigma_{res}\right)}{S_u}\right\} \qquad (3)$$

When the normal load ratio, R (= $\sigma_{min}/\sigma_{max}$) becomes zero, then $\sigma_{mean} = \sigma_{max}/2$. Therefore, the stress amplitude, which considers welding residual stress, can be written as

$$\sigma_{a-res} = S_e\left\{\frac{2S_u - \left(\sigma_{max} + 2\sigma_{res}\right)}{2S_u}\right\} \qquad (4)$$

Load Range (ΔP)–Fatigue Life (N_f) Relation

Specimens and the Testing Method

Dimensions and shapes of the specimens were the same as those in the FEA models. The welding conditions followed were from the recommendation of RWMA (Ref. 13) class-C, illustrated in Table 3. The diameter of the electrode used for spot-welding was 6 mm, a typical size for an actual application. The fatigue testing machine used is a servo-hydraulic power system (MTS, capability 98 kN). Fatigue tests, such as tensile shear (TS) type specimens, are generally conducted with simple plate grips (Refs. 14–15). However, in the case of IB-type spot-welded joints subjected to tension-shear load, the simple grip cannot be used due to in-plane bending deformation of spot-welded lap joints. Thus, in the present test, the pin joint grips were used to remove the effects of in-plane bending deformation and force (Ref. 16).

Fatigue tests were conducted under the following conditions: frequency (f) was 25 Hz, cyclic loading form was Sine wave, and normal load ratio was 0 since it is known that the influence of the frequency for fatigue strength at room temperature and in air is negligible (Refs. 16, 17). The number of cycles to failure was determined as the cycles when a fatigue crack appeared on the outer surface of the specimen and when its length was equal to nugget diameter. Fatigue limit of each specimen was determined as the load that did not initiate a crack at 10^7 cycles.

Fatigue Test

The fatigue test results for various IB-type spot-welded joints are shown in Fig. 9 as ΔP-N_f relations. The influence of the geometrical factors on fatigue strength can be observed. In higher loads and shorter life ranges, the influence of the plate thickness is not clearly observed due to the complicated deformation characteristics of the thin plate. However, in lower loads and longer life ranges, it is clearly revealed. The fatigue strength considerably increases with the plate thickness under the same loading condition due to the increase of bending rigidity of the plate. For the same thickness, the fatigue life decreases with the joint angle of the specimen due to the fact that torque of the weld nugget by in-plane bending deformation linearly increases with the joint angle. However, the influence of the plate width on fatigue strength is not clearly identified. Since the data of the ΔP-N_f relations are widely scattered by the influence of geometrical factors, it is difficult to determine the fatigue design criterion even with a slight change of the design.

Fatigue Strength Assessment Considering Welding Residual Stresses

Many investigators have numerically and experimentally attempted to establish a reasonable fatigue design method for spot-welded lap joints. Some insightful results can be found in such publications as *Engineering Fracture Mechanics, Fatigue and Fracture of Engineering Materials and Structures, Journal of JSAE,* and *JSAE Review*. However, it is still difficult to find an approach considering welding residual stresses in fatigue strength assessments. Therefore, the stress amplitude ($\sigma_{a\text{-}res}$), which considered welding residual stress, was employed to establish a reasonable fatigue strength assessment method for spot welds with various dimensions and shapes.

Figure 10 shows the $\sigma_{a\text{-}res}$-N_f relation of IB-type spot-welded lap joints with various dimensions and shapes under tensile shear loading. Figure 11 shows the comparison between the fatigue strengths represented by stress amplitudes with and without consideration of welding residual stresses. Fatigue strengths from the stress amplitude range that neglect welding residual stresses are much higher than those that consider welding residual stresses. From Fig. 10, the fatigue strength at fatigue limit was around 32 MPa. This value is about 25% lower than that neglecting welding residual stresses. This indicates that fatigue strength of IB-type spot-welded joints could be greatly overestimated by neglecting welding residual stresses. Therefore, for determining more reasonable fatigue design criterion of the spot-welded structures, the welding residual stresses generated in the welding process should be considered in fatigue strength assessment.

Conclusions

The following conclusions are made in this study:

1) Welding residual stresses of spot-welded joints were calculated by the nonlinear FEA method and compared with the experimentally measured values by the X-ray diffraction method. The residual stress distributions show reasonable agreement between the calculations and measurements.

2) To develop a reasonable fatigue strength assessment method of spot-welded joints with various dimensions and shapes, a stress amplitude that takes into consideration welding residual stress ($\sigma_{a\text{-}res}$) was proposed. In this study, it is shown the proposed stress amplitude ($\sigma_{a\text{-}res}$) can provide a systematic and accurate evaluation of fatigue strength of spot-welded joints with various dimensions and shapes.

3) The fatigue strength at a fatigue limit that considers welding residual stress is about 25% lower than that without consideration of welding residual stresses.

References

1. Hujimoto, M. O., Mori, S. K., and Ojima, M. 1985. Modeling of automobile structure members and research objects. *JSAE Symposium*, JSAE, pp. 20–26.
2. JSAE. 1987. *Databook Fatigue Data of Spot-Welded Joints.* JSAE, pp. 12–185.
3. Bae, D. H. 1991. Fracture mechanical fatigue strength evaluation of IB-type-spot welded lap joint under tension shear load. *Journal of KSAE* 13(5): 42–50.
4. Radaj, D., and Zhang, S. 1995. Geometrically nonlinear behavior of spot-welded joint in tensile and compressive shear loading. *Journal of Engineering Fracture Mechanics* 51(2): 281–294.
5. Radaj, D., Zheng, Z., and Moehrmann, W. 1990. Local stress parameter at the spot weld of various specimens. *Journal of Engineering Fracture Mechanics* 37(5): 993–951.
6. Huh, H., and Kang, W. J. 1997. Electrothermal analysis of the electric resistance spot welding process by a 3-D finite element method. *Journal of Material Processing Technology* 63 (1–3): 672–677.
7. Tsai, C. L., Dickinson, D., and Jammal, O. A. 1990. Study of nugget formation in resistance spot welding using finite element method. *Recent Trends in Welding Science and Technology.* Eds. S. A. Davis and J. M. Vitek, pp. 43–53. ASM International, Materials Park, Ohio.
8. Anastassiou, M., Babbit, M., and Lebrun, J. L. 1990. Residual stress and microstructure distribution in spot-welded steel sheet: Relation with fatigue behavior. *Material Science and Engineering* A125: 141–156.
9. Nied, H. A. 1984. The finite element modeling of the resistance spot welding process. *Welding Journal* 63(4): 123-s to 132-s.
10. Kim, E. W., and Eager, T. W. 1989. Measurement of transient temperature response during resistance spot welding. *Welding Journal* 68(8): 303-s to 311-s.
11. Niemi, E. 1995. *Stress Determination for Fatigue Analysis of Welded Components*. England: Abington Publishing pp. 3–25.
12. Goldsmith, A. 1961. *Handbook of Thermo Physical Properties of Solid Materials.* Revised ed. II. The MacMillan Co, pp. 28–56.
13. RWMA, 1981. *Residual Spot Welding Manual* 1: 119–143.
14. Tomioka, N., Niisawa, J., and Bae, D. H. 1988. Theoretical analysis of stress distribution of single spot-welded lap joint under tension-shear load. *Journal of JSAE* 39: 105–112.
15. Bae, D. H., Niisawa, J., and Koiso, A. 1988. On stress distribution and fatigue strength of single elliptical spot-welded lap joint under tension shear load. *JSAE Review* 9 (4): 86–91.
16. Sohn, I. S. 1998. A study on the fatigue design method and expert system development for thin steel sheet spot welded lap joint. Ph. D. dissertation. SungKyunKwan University, S. Korea.
17. Shigley, J.E., and Mischke, C. R. 1989. *Mechanical Engineering Design*. 5th ed., McGraw-Hill, pp. 286–288.